

Patch Antenna with Slots and Sar reduced through AMC

Geraldo Fulgêncio de Oliveira Neto¹, Álvaro Augusto Almeida de Salles²

¹Programa de Pós-Graduação em Engenharia Elétrica, Universidade Federal do Rio Grande do Sul, UFRGS, Porto Alegre, RS, Brasil

geraldo.fulgencio@ufrgs.br

²Departamento de Engenharia Elétrica, Universidade Federal do Rio Grande do Sul, UFRGS, Porto Alegre, RS, Brasil

aasalles@ufrgs.br

Received: 04 Dec 2021,

Received in revised form: 13 Jan 2022,

Accepted: 20 Jan 2022,

Available online: 31 Jan 2022

©2022 The Author(s). Published by AI
Publication. This is an open access article
under the CC BY license

(<https://creativecommons.org/licenses/by/4.0/>).

Keywords— Slotted patch antenna, 5G
antennas with AMC, SAR reduction.

Abstract— This study proposes a system consisting of a “patch” [1] dual-band antenna [2] with slots, dimensioned for 5G applications. In this device an AMC (“Artificial Magnetic Conductor”) structure was inserted in order to improve the operating characteristics. The AMC plane [3] is formed using a 2 x 2 matrix of unit cells, each with a U-shape and a reconfigurable element. The results compared with an antenna without AMC indicate that the system provides SAR reduction, directivity improvement and gain increase to be discussed in the text.

I. INTRODUCTION

5G is the latest mobile network technology and has the potential to make our lives smarter, safer and more efficient. As the next generation of network technology for mobile applications, 5G offers exciting opportunities in healthcare, education and agriculture. In this way 5G systems promise to drastically change our lives after their implementation, bringing features such as increased speed compared to 4G, increased bandwidth, reduced latency and the explosion in the consumption of interconnected equipment with previously unimaginable amounts of users and new applications. However, the operating range and the expansion of the number of antennas involved, combined to the large-scale use of equipment, increase the risks related to human exposure to non-ionizing radiation. When placed close to the body, an antenna with high radiation or omnidirectional pattern such as a dipole antenna tends to produce increased electromagnetic absorption in the human body due to its proximity during operation. This results in a high Specific Absorption Rate (SAR) [4] value, which potentially affects

the tissues of the human body. The American National Standards Institute (ANSI) and the International Commission on Non-Ionizing Radiation Protection (ICNIRP) have regulated that exposure to human tissue is limited to 1.6 W / kg on average per 1g of tissue and 2 W / kg per 10 g of tissue, respectively. In view of this demand, this work describes a dual-band planar antenna within the frequency range intended for the installation of 5G in Brazil, (as approved by the ANATEL Regulatory Agency) together with an AMC type metamaterial (“Artificial Magnetic Conductor”) [3] designed to reduce the SAR Specific Absorption Rate and further improve the antenna directivity.

II. MICROSTRIP ANTENNA

With the evolution of printed circuit production technology and the ease of construction, microstrip antennas have been used in various equipments. Their relevance is determined by being adaptable to the environment, moldable to curved surfaces, inexpensive and mechanically robust, particularly when mounted on rigid surfaces. Such antennas can be installed in different types of equipments or means of transport such as: aircraft,

satellites, missiles, radar, automobiles, cell phones, demonstrating their enormous versatility [1]. This type of antenna adds competitive advantage in certain applications. The possibility of multiple band and the convenient radiation diagram can be elective differential at the time of manufacture. This also happens with the other characteristics of the microstrip antenna, such as: smaller dimensions, reduced weight, ease of fabrication, low cost, easy adaptation to the surfaces of the devices, good integration with other types of circuits, etc. The modeling of the antenna is directly related to what is intended to be achieved in the final result, such as an antenna with a good bandwidth to be applied to a wireless communication device or with a narrow frequency band to be applied to a frequency filter. Since the beginning of wireless communications, which date from the end of the 19th century, to the present, the increase in research was remarkable and an unexpected evolution in these systems was observed in that period. The advent of wireless telegraph and the use of electromagnetic transmission as a means of information transmission resulted in a significant improvement in the research of components for the infrastructure of communication systems. Among the researched components, one of the main elements that gained prominence, due to its importance, were the radiating elements, popularly known as antennas.

The Institute of Electrical and Electronic Engineers (IEEE) defines the term “antenna” as “that part of a transmitting or receiving system that is designed to radiate or receive electromagnetic waves”. In other words, an antenna is an intermediary structure between free space and the transmitting or receiving electronic device. The connection between the electronic device and the antenna is made through a guiding device, which can take the form of a coaxial cable, a waveguide or a flat transmission line (microstrip type, for example). When electromagnetic energy is transported from the transmission source to the antenna, the antenna is called transmitter, when energy is transported from the antenna to the receiver, then it is a receiving antenna [1].

Since many years, several models have been developed which have emerged for diverse applications. Reflector antennas, loop antennas, short dipoles and horns are among the most common models.

However, in 1953 Deschamps and Sichak proposed a new model in the development of resonator elements. In their work, the construction of low-cost planar antennas in microstrip technology was proposed. The works by Munson (1974) and Kerr (1978) consolidated Deschamps' idea and added new techniques for the construction of microstrip antennas [5].

In cases where space or weight is limited, the use of planar structures as a radiating element for electromagnetic waves becomes attractive. Such conditions are very convenient in, for example: airplanes, satellites, Vant's and mobile devices.

In addition to these characteristics, microstrip type antennas have greater flexibility for adjustments in electromagnetic parameters such as resonance frequency, polarization, radiation pattern, impedance matching and bandwidth [1].

A microstrip antenna consists of two minimally thick metallic layers separated by a dielectric layer, the substrate. These layers are arranged in a planar structure.

The radiating element above the substrate is called "Patch", and it is through this element that the waves are transferred from the antenna medium and radiate to the free space. The patch structure has a direct relationship with the distribution of current and electromagnetic fields in the substrate.

A metal ground plane is placed below the substrate and it works as a ground for the antenna, in addition to acting as a reflector, thus reducing the side and secondary lobes [1]. The structure of a microstrip patch antenna is represented in Fig. 1.

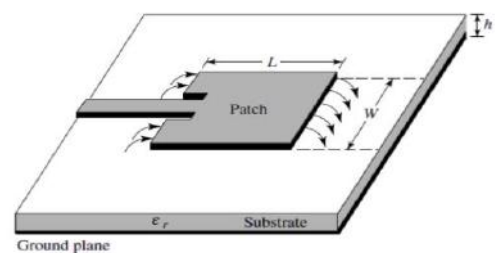


Fig.1 - Representation of a Microstrip Antenna
Source: Adapted from Balanis (2016)

Where, h is the height of the substrate, ϵ_r is the relative permittivity of the dielectric and W and L correspond, respectively, to the width and the length of the rectangular patch.

The layout of the antenna can have different forms. Each of them corresponds to a different mathematical model for the analysis the electromagnetic behavior of the antenna.

The most common shapes, such as the rectangular and circular patch are used more frequently in research and development where the shape is not a fundamental element in the variation of the antenna performance parameters [1].

In general, the possible antenna shapes play important roles in more specific applications, in the case of the rectangular patch will have more general applications. For example, the controlled insertion of slits in its radiating

element can change the component into an antenna dedicated to specific applications. This situation is one of the objects of study in this work.

The intermediate layer of the patch antenna, the substrate, is a fundamental element for antenna design. The physical characteristics of the substrate directly influence some antenna parameters, such as its radiation efficiency, size, bandwidth, etc... Among the materials desired for improved performance, those with greater thickness and lower dielectric constant are preferred, at the cost of one larger device dimensions [1].

However, if the element size is a key condition for the system, thinner substrates with a higher dielectric constant are indicated, with considerably device dimension reduction.

2.1 Antenna Performance Parameters.

When the electromagnetic behavior of the antennas is considered, it is possible to verify that there is a significant dependence between the performance and its main parameters. [6]

As far as microstrip antennas are concerned, the main limitation is the bandwidth. The main reason for the small thickness used is the attempt to minimize the effect of electromagnetic waves that propagate inside the dielectric.

As an opposite result, if we increase the thickness (height) of the antenna's dielectric substrate, the bandwidth increases. However an adverse effect is produced, since the increase in the thickness of the dielectric produces surface waves, which distorts the radiation pattern and usually reduces the radiation efficiency when reaching the edge of the substrate.

Also, the antenna feeding techniques when increasing the substrate thickness are also impaired [6].

Among others, two parameters are of great relevance during the design of an antenna : One of them is the antenna input impedance, associated with the return loss of the power incident on its input. This parameter facilitates the understanding of how the antenna is linked to the supply structure in a given frequency range. The second parameter is the radiation pattern, which represents how the electromagnetic energy is distributed by the antenna in the space.

Regarding radiation there are other dependent parameters, for example, it can be mentioned: the front-to-back, ratio, the side lobes, the level of cross polarization for antennas with linear polarization, the gain, the directivity, the efficiency and the axis ratio for circular polarization antennas.

In order to establish the application of the antenna and determine its performance, this section will analyze characteristics such as: gain, return loss, radiation pattern, polarization and bandwidth.

2.1.1 Radiation Pattern

The radiation pattern of an antenna is defined by Balanis (2011) as a mathematical function or graphical representation of the radiation properties of an antenna as a function of spatial coordinates θ (elevation angle) and ϕ (azimuth angle). The determination of the radiation pattern of an antenna is obtained from the intensity in the far field of the antenna [7].

Figure 2 represents the coordinate system for the radiation pattern of an antenna.

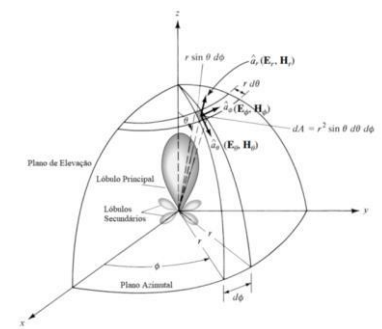


Fig.2 - Microstrip Antenna Radiation Pattern

Source: Adapted from Balanis (2016)

The representation of the radiation pattern of an antenna can be done in either two or three dimensions, the first being a representation of the cut planes performed in the 3D diagram.

The vertical or elevation plane is represented by θ and normally corresponds to 0° or 90° , while the horizontal or azimuthal plane is represented by ϕ and for better visualization is defined as 90° [1].

The radiation pattern and allow to characterize the performance of an antenna. Then, it is possible to estimate e.g., the directivity, analyzing the main lobe as well as the side and rear lobes.

There is no ideal relationship between these lobes for all antennas, allowing the division into two main classes, : omnidirectional antennas and directives, where each one has different applications, depending on the desired coverage, [1].

2.1.2 Directivity, Gain and Efficiency

According to Balanis [1] directivity is given as the ratio between the radiation intensity in one direction and the average of the radiation intensities in all directions, where the radiation intensity of an isotropic source is given by:

$$U_0 = P_{\text{rad}} / 4 \pi$$

Relating the radiation intensities according to the definition of directivity, we have:

$$D = U / U_0$$

Soon,

$$D = 4\pi U / P_{\text{rad}}$$

It is observed from the previous equation that for an isotropic antenna the directivity has an unitary value, η_s the radiated intensity in any direction is constant.

The calculation of the directivity must be associated with the efficiency of the antenna in question, as the previous equations disregard the resistive and the dielectric losses [56].

According to Balanis [1], the efficiency of an antenna is given by:

$$\eta_0 = \eta_{\text{ed}} (1 - \eta_r)^2 \quad [1]$$

Equation 1 presented relates the total efficiency η_0 with the radiation (η_{ed}) and reflection (η_r) efficiencies. The association of the directivity with the efficiency of an antenna provides a third parameter, the gain, which is also a of fundamental importance for application in wireless communication links. Balanis [1] states that the gain of an antenna is the relationship between the intensity radiated in one direction and the intensity obtained if all the input power (P_{in}) were radiated by an isotropic source.

$$U_0 = P_{\text{in}} / 4 \pi$$

Therefore, the gain is given by

$$G = 4 \pi U / P_{\text{in}}$$

It is observed by the similarity between the equations, the relationship between the gain and the directivity.

These two parameters differ because the antenna efficiency is not unitary, so that not all the input power (P_{in}) is converted into radiated power (P_{rad}). Thus, the following equation can be written.

$$P_{\text{rad}} = \eta_{\text{ed}} * P_{\text{in}} \quad [2]$$

Substituting [2] in the gain equation, one obtains

$$G = \eta_{\text{ed}} 4\pi U / P_{\text{rad}}$$

Thus,

$$G = \eta_{\text{ed}} D$$

This equation optimizes the gain calculation by eliminating the reflection efficiency variable (η_r), which can be different from 1 (one) when there is no perfect impedance matching. To estimate a value to the gain, then the following equation can be used

$$G = \eta_0 D$$

2.1.3 Return Loss (S_{11})

As already mentioned, the return loss R_L is one of the main design parameters of an antenna, as it is a measure that indicates the possibility of the prototype working correctly when built. This parameter determines the relationship between the incident and reflected wave in the direction of the load [7]. Return loss can be calculated as in Equation 3.11.

$$R_L = -20 \cdot \text{Log} |\rho|$$

Where ρ is the reflection coefficient.

It is also possible to obtain the return loss through the analysis of the scattering matrix. Pozar [7] defines this method as the most suitable to derive the relationships between transmission line and load.

III. METAMATERIALS

The term metamaterial can be considered as an artificial compound which exhibits electromagnetic properties not found in natural materials. Also known as left-handed material (LHM), electromagnetic bandgap material (EBG), artificial magnetic conductor (AMC), high impedance surface (HIS), etc.

Metamaterials can also be conceptualized as periodic structures, dielectric or metallic, which behave like homogeneous materials. This periodicity leads to resonant structures that may seem incompatible with a broadband application.

To design an unidirectional antenna, which is the case on many platforms, the antenna must radiate outward. The antenna is usually supported by a reflector or absorption cavity.

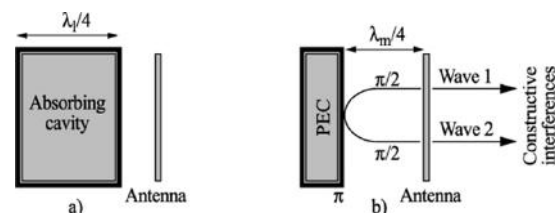


Fig.3 - Unidirectional antenna above the cavity (a); and PEC (perfect electrical conductor) (b)

The solution with the absorption cavity is simple, but half of the radiation is lost (Figure 3a), as all the energy radiated towards it is absorbed. Absorbent materials are heavy and features are difficult to reproduce. Furthermore, the has dimensions close to a quarter wavelength at the lowest operating frequency, which becomes a problem at low frequency applications.

Another efficient technique is to use a reflector composed of a perfect electrical conductor (PEC) to reflect the back radiation (Figure 3b). This technique is ideal in mid-bandwidth, where the constructive interference phenomenon is achieved by placing the reflector at a quarter wavelength (at the center frequency) of the antenna. This solution is inherently bandwidth-limited and can rarely exceed an octave [1].

Among the objectives of this work, it is intended to conceive the combination of directivity improvement, SAR reduction and compactness. Therefore, metamaterials as the artificial magnetic conductors (AMC) have relevant characteristics. While in a conductive metal the reflected wave produce a phase shift of π , the artificial magnetic conductors do not introduce a phase shift (Figure 4).

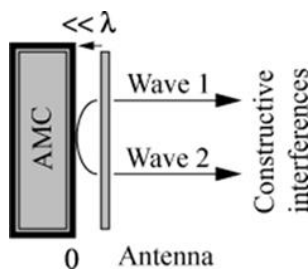


Fig.4 - Unidirectional antenna with AMC

3.1 The design of the AMC unit cell

As a computational validation criterion, initially, a unit cell with square metallic patch is implemented, whose design parameters used are similar to those obtained in the work of Zhang [8].

However, the implementation made here differs basically in terms of the numerical method applied to obtain the phase of the reflection coefficient at the AMC.

In Zhang's work, the study is performed in the time domain using the FDTD (Time Domain Finite Difference Method), while here, the simulations were performed in the frequency domain using the FEM (Finite Element Method), included in a commercial CST software.

In this work, the unit cell implementation consists of a model based on the Bloch-Floquet theory [9]. Essentially, the unit cell of the AMC structure has periodic boundary conditions (PBCs) on its four sides, thus modeling an infinite periodic surface, as it is shown in Figure 5. For simplicity, the metallic patch (in orange on top) and the ground plane (in orange at the bottom) are specified as perfect electrical conductors (PEC).

The space between the metallic radiating element and the earth plane is filled with a dielectric substrate. To excite the structure, a probe is placed, at half-wavelength ($\lambda/2$),

above the metallic track and a plane wave linearly polarized in the z direction is produced.

As in this work the frequency domain is used, different wavelengths are used to excite the AMC surface, representing a frequency window (interval). In the text, λ_i and λ_f will be the initial and final wavelengths, respectively, corresponding to the initial and final excitation frequency, f_i and f_f .

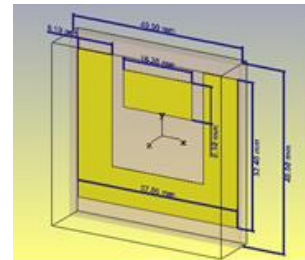


Fig.5 - Unit cell design.

IV. OPTIMIZATION ALGORITHMS FOR THE ANTENNA DESIGN.

From a structural point of view, the frequency response of microstrip antennas depends on the dimensions and geometries involved in the design. Also, the AMC unit cell, including its periodicity, the dielectric substrate used, the type of element used and its geometric shape are important [10]. Several geometric shapes for the those elements have already been described in the literature. Some of these elements are shown in Figure 6.

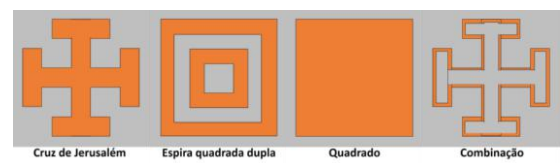


Fig.6: Typical geometries of the elements of a FSS (Frequency Selective Surface). Source: adapted from reference (10).

Although these geometries are simple, more complex shapes include fractal geometries [11; 12; 13]. In the antenna and in the AMC design described in this work, the evolutionary algorithm CMA-ES was used. In order to validate and to improve the optimization algorithms, all new optimization routines, based on evolutionary theories, were checked via test functions. These functions, initially, are single-purpose, in order to facilitate the study.

4.1 ADAPTATION OF THE COVARIANCE MATRIX - Evolution Strategies (CMA-ES)

The CMA-ES algorithm was first proposed by Nikolaus Hansen in 2001 [14]. It is a bio-inspired optimization algorithm. The CMA-ES has a candidate population distribution model (Multivariate Parameterized Normal Distribution) to explore the project space [15]. It is based on the selection and adaptation strategy of the sample population, preserving and modifying the parameters of the strategy, the convergence property of previous generations (Covariance Matrix), using knowledge in the generation of the next generation population. In each generation, the parent for the next generation is calculated as a weighted average of λ candidates selected from μ descendants generated in that generation using a selection (λ, μ) .

The next-generation population is generated by sampling a multivariate normal distribution of the Covariance Matrix with the variance in generation g over the generation mean $MN(M(g), (\sigma(g))^2 C(g))$ [16] [3].

The step size $\sigma(g)$ determines the overall variance of the mutation in generation g .

The variable property of step size σ in each generation plays a vital role in controlling premature convergence and convergence close to global optimals.

CMA-ES works through a cycle of steps depicted in Figure 7.

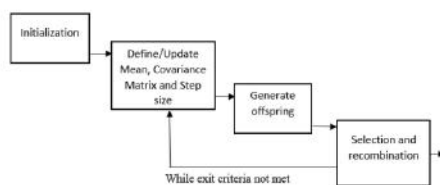


Figure 1. Evolutionary strategies life cycle.

Fig.7- Operation of the CMA-ES through a cycle of steps.

The evolutionary strategy based on the adaptation of the covariance matrix, CMA-ES, proved to be superior to other evolutionary strategies. The fact that it is a model with well-defined mathematical functions makes the algorithm easy to handle when it comes to changing parameters.

V. SAR AND ELECTROMAGNETIC ENERGY ABSORPTION

In the human body, each type of biological tissue has different levels of absorption of electromagnetic energy.

Then, the concept of specific absorption rate (SAR - Specific Absorption Rate) was created in order to quantify the absorbed energy, specifically, in different irradiated tissues [17].

Specific Absorption Rate (SAR) is the rate of energy absorption by the body tissues, in specific watts per kilogram (W/kg).

Therefore, it is the dosimetric parameter used to establish limits to the absorption of radiation due to non-ionizing electromagnetic fields. The concept of dose, energy (or power) absorbed per unit of mass, was developed to set the limits for non ionizing radiation.

When defining the SAR, an attempt was made to establish a measurement unit (dose) correlated with the effects of the body temperature increase.

SAR values depend on incident field parameters, such as: frequency, intensity, polarization and source-object configuration (near or far field); characteristics of the exposed body such as size, internal and external geometry; dielectric properties of different tissues and, also, reflective effects of the soil and other objects close to the exposed body. When the human body axis is parallel to the electric field vector, and under plane wave exposure condition, whole body SAR reaches maximum values. In practice, there is no way to measure SAR values directly on humans. To analyze the effect, computational simulations are used in order to calculate it as in the case of this work. Also, other quantities can be used to assess exposure to electromagnetic energies, such as the electric and the magnetic field intensities, as well as the power density.

Exposure to more intense fields, producing SAR values greater than 4 W/kg, can exceed the body's thermoregulatory capacity and produce tissue-damage.

5.1 EMF Exposure Limits

ICNIRP, the acronym in English of the International Commission on Non-Ionizing Radiation Protection, established recommendations to limit non-ionizing radiation, which are adopted by most countries in the world, including Brazil through Anatel. [18]

Exposure limits are based on the average human body SAR determined under the following conditions:

- Flat wave with the man standing, parallel to the incident electric field, which represents a situation of greater absorption, except in relation to a few special cases.
- SAR should be averaged over a 6-minute time period in order to maintain the relationship between absorbed power and induced heating (increase on the tissue temperature due to the EMF absorption).

As the threshold for irreversible effects is above 4 W/kg, ICNIRP has established exposure levels for professionals (occupational) and the general public with safety factors of 10 and 50 times the threshold, respectively.

SAR factor of safety

Irreversible thermal effects > 4 W/kg

Table 2 - ICNIRP established exposure levels for professionals in the field (occupational) and the general public with safety factors.

| | | |
|----------------------|-----------|----|
| Occupational Limit | 0,4 W/kg | 10 |
| General Public Limit | 0,08 W/kg | 50 |

It is important to mention that other EMF exposure effects (such as the "non-thermal effects") are not considered in the ICNIRP recommendations.

VI. PROGRESS OF RESEARCH

In the antenna design, the adequate parameters were obtained through computational analysis, in which the radiating element is divided into sectors of interest based on the analysis of the distribution of surface current densities and, in these sectors, the Balanis equations were applied [1] to determine the resonant bands.

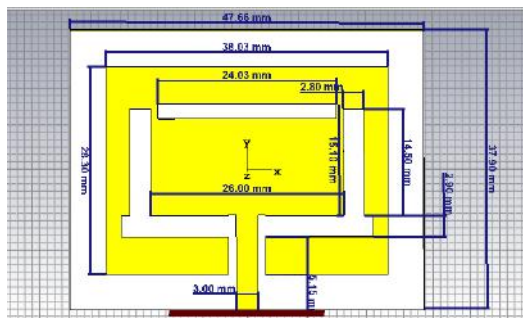


Fig.7 - Dimensions of the produced antenna.

During the implementation of the design, the behavior of different antenna formats was verified and, finally, the need to create an original layout and develop a methodology in order to meet the requirements was defined. Once the "patch" antenna layout was identified, a methodology based on an evolutionary algorithm (CMA-ES) was implemented to determine the most suitable placement of the slots. The CMA-ES algorithm was simulated using a population of variables consisting of the width of the radiating element, length and positioning of the mobile slit, thus obtaining the resonances at the desired frequencies. This implementation was performed using a planar antenna [1] with the insertion of 5 slits (four fixed and one mobile). As shown in Figure 7, the variation of the

movable slit coordinates produced the necessary effect to obtain the double band [2] in the bands assigned for 5G.

The radiating element was developed with the insertion of slits in order to produce double resonance. After creating the layout, the position of the overslot used was inserted and changed (with the implementation of the CMA-ES algorithm) to facilitate the adjustment of the frequency ranges of interest. The structure is based on a Series Band Pass filter:

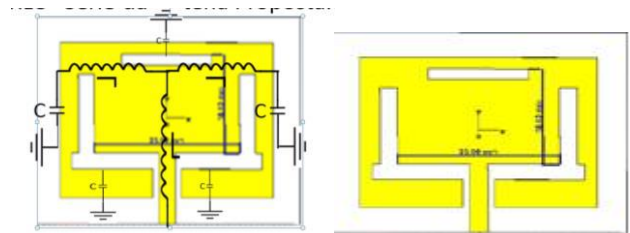


Fig.8 - Antenna geometry and simulation of a Series Bandpass Filter:

Component distribution aspect for modeling in RLC – Proposed Antenna. Based on the analysis of RLC electrical circuits, the angular frequency was calculated.

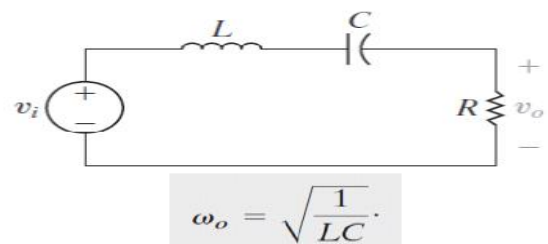


Fig.9 - Antenna equivalent circuit.

Antenna calculation based on Series RLC Band Pass Filter. The initial design specifications considered the target resonance frequencies (f_r), the relative permittivity (ϵ_r) = 4.7 and the dielectric thickness (h) = 1.6 mm

$$L_p = \frac{c}{2.f_r \sqrt{\epsilon_r}} - 2\Delta L \quad [1]$$

$$W_p = \frac{c}{2.f_r} \cdot \sqrt{\frac{2}{\epsilon_r + 1}} \quad [2]$$

From these, the frequencies f_{r1} and f_{r2} were calculated [1] based on the parameters L and W and, with the same parameters, two antennas were simulated. The FR4 substrate was used. The CST Studio Suite software was employed. This is a software package for high-performance 3D Electromagnetic analysis allowing the design, the analyses and the optimization of

electromagnetic (EM) components and systems. This simulation package offers analysis of the performance and the efficiency of antennas and filters, the compatibility and the electromagnetic interference (EMC / EMI), as well as the exposure of the human body to EM fields, electromechanical effects in motors and generators, and thermal effects in high power devices. CST Studio Suite is used in engineering to optimize device performance by identifying compliance issues early in the design process and reducing the number of physical prototypes needed and the risk of test failures and recalls.

After the simulation and obtaining the parameters close to the two desired resonances, the CMA-ES algorithm was implemented in the design procedure in order to improve the performance.

7.1 Implementation of metamaterials on the antenna

Metamaterials also known as high impedance surfaces (HIS) have relevant properties in controlling the propagation of electromagnetic waves. Two of these properties are of special interest. First, they can behave like perfect magnetic conductors, so the parallel currents in the image appear in-phase rather than out-of-phase. This feature allows efficient radiation for antennas placed parallel and close to the surface. Second, they limit the propagation of electromagnetic waves in certain frequency bands [19] ("electromagnetic bandgap" or EBG), so that there is no multipath interference and the radiation patterns are smoother.

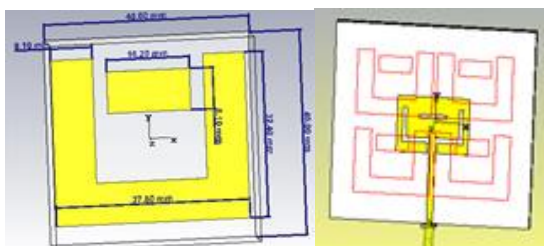


Fig.10 - (a)AMC unit cell appearance. (b) AMC 2X2 matrix.

Fig. 10 (a) illustrates the AMC cell developed in this research and figure (b) shows the cell matrix proposed in order to minimize the effect of SAR. The developed antenna structure consists of five layers distributed as follows: a layer for ground plane (the lowest layer), followed by two substrate layers (FR4) and a layer consisting of the AMC between them. Finally, a layer for the radiant element placed on the top.

To improve the directivity and reduce the SAR, a solution composed of artificial magnetic conductors (AMC)[6] was developed, also known as high impedance surfaces (HIS) or metamaterials. As highlighted in item 6, these

elements have properties in controlling the propagation of electromagnetic waves. Figure 11 shows the Reflection Diagram relating to the AMC unit cell.

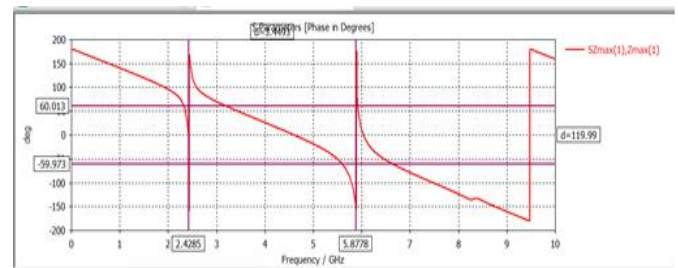


Fig.11 - Unit cell phase diagram

VII. RESULTS

As explained above, in the proposed antenna a metamaterial structure of the AMC type ("Artificial Magnetic Conductor") was inserted. The AMC plane [3] is formed using a 2 x 2 matrix of unit cells, each U-shaped, and a movable element for adjustment ("overslot").

The radiant element was developed with the slit insert.

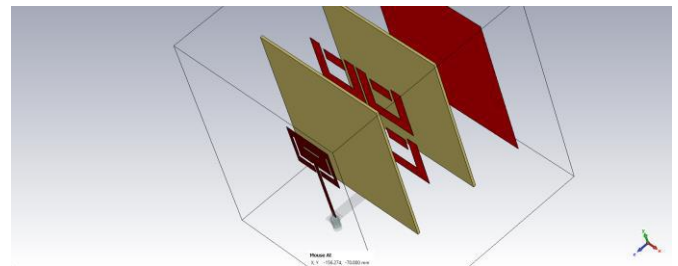


Fig.12 - (a) Overview of the exploded antenna.

In this way, an improvement in the directivity and a reduction in the SAR was obtained. The Microstrip Antenna System with slots[20] + AMC and ground plane (Figure 11). The figures below show results produced in the proposed antenna. For comparison purposes, screens with and without AMC were selected for the following characteristics: Return loss as a function of frequency (S_{11}), gain, radiation diagrams and SAR.

Antenna Patch with slots and AMC.

As described in item 6, the antenna structure developed was presented in the previous item and consists of five layers. In order to analyse the behavior of the antenna and its specific absorption rate (SAR) a phantom [21,22] with electrical characteristics similar to the human body was used. The antenna was positioned 6 mm apart at the center of the phantom.

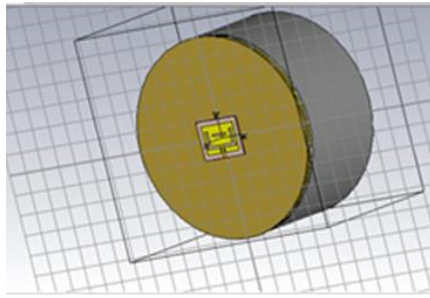


Fig.13 - Antenna was positioned at the center of the phantom.

Initially, simulations of the patch antenna were carried out without the insertion of AMC and the SAR screens obtained with the phantom were collected. The simulated S_{11} , directivity, gain and SAR at 2.4 GHz are shown in Figures from 14 to 22.

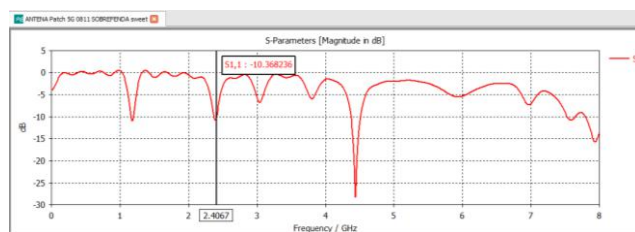


Fig.14 – S_{11} Antenna Return Loss without the AMC

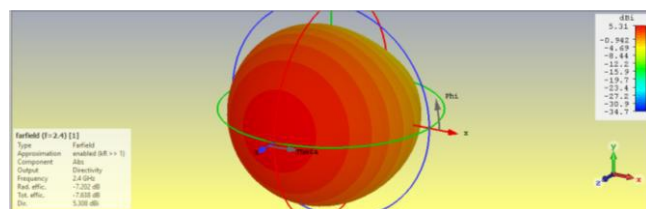


Fig.15 – Radiation pattern at 2.4 GHz without the AMC

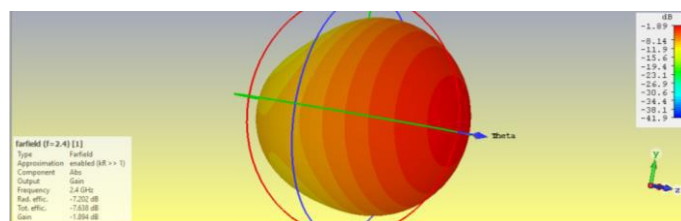


Fig.16 – Radiation pattern at 2.4 GHz without the AMC.

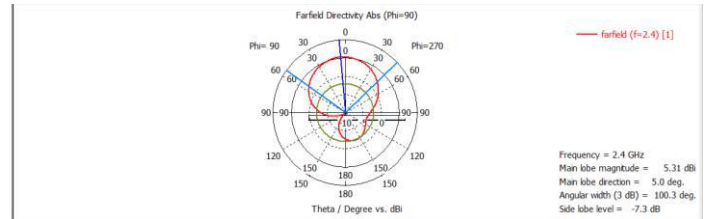


Fig.17 – 2D Radiation pattern at 2.4 GHz without the AMC.

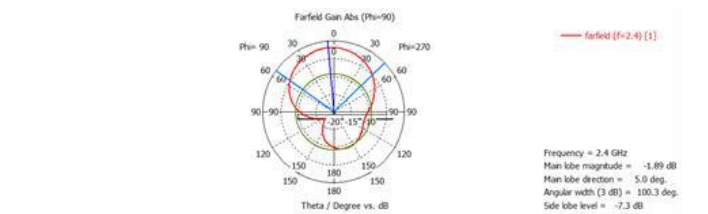


Fig.18 – Radiation pattern at 2.4 GHz without the AMC.

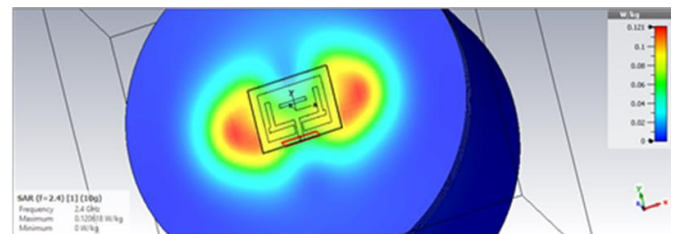


Fig.19 – SAR 10g at 2.4 GHz without the AMC.

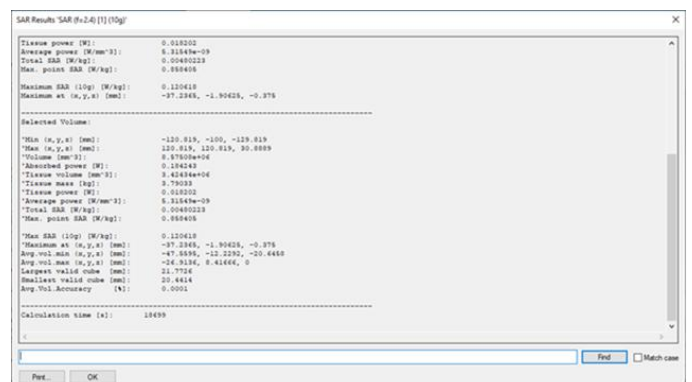


Fig.20 – 10g SAR report at 2.4 GHz

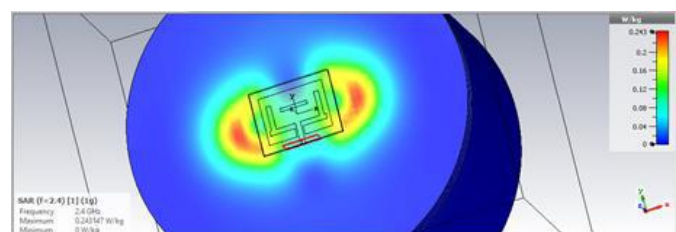


Fig.21 – SAR 1g at 2.4 GHz without the AMC

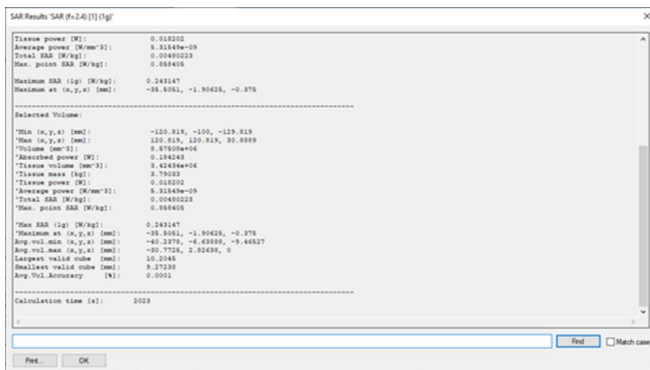


Fig.22 – SAR 1g report at 2.4 GHz frequency

In the second stage of the research the metamaterial structure (AMC) was introduced into the patch antenna and, after the simulation, the return loss S_{11} was obtained.

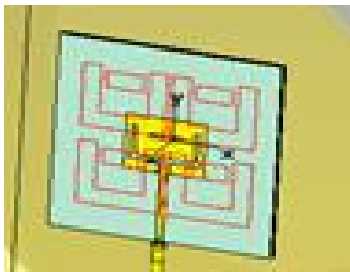
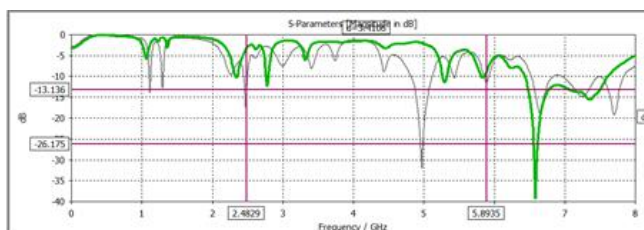


Fig.23 - Antenna and the AMC

Fig.24 – S_{11} Antenna and AMC Return Loss

Radiation pattern at 2.4 GHz were obtained from the simulation.

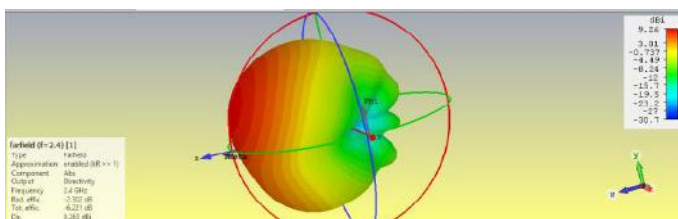


Figure 25 - Radiation pattern at 2.4 GHz with the AMC

Antenna gain with AMC at 2.4 GHz frequency.

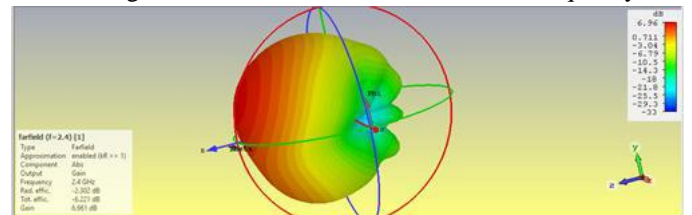


Figure 26 – Radiation pattern at 2.4 GHz with the AMC.

Front to back ratio

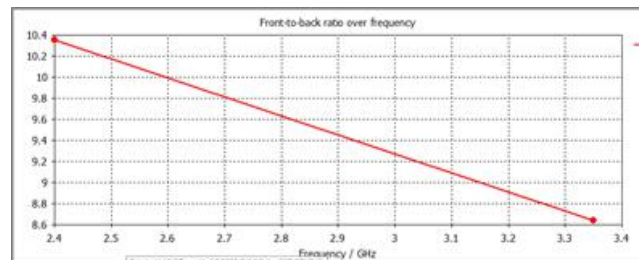


Fig.27 – Front to back ratio at 2.4 GHz

From the simulation, the radiation pattern and DIRECTIVITY directivity at 2.4 GHz were obtained, Also, 1 g SAR was simulated for the antenna with the 2x2 AMC.

SAR 1g

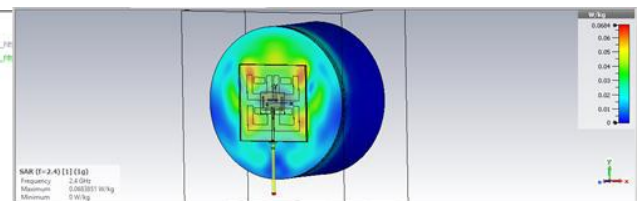


Fig.28 – SAR 1g at 2.4 GHz with the AMC

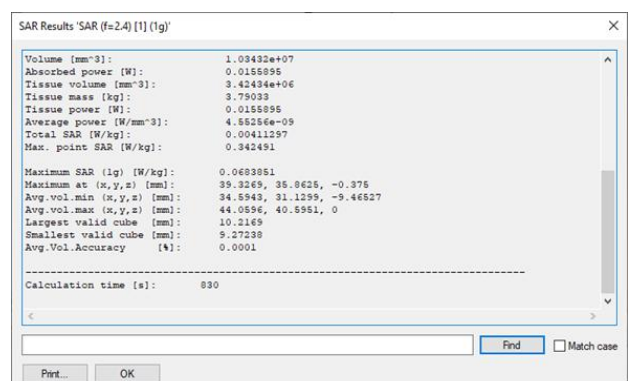


Fig.29 – SAR 10g report at 2.4 GHz

SAR 10g

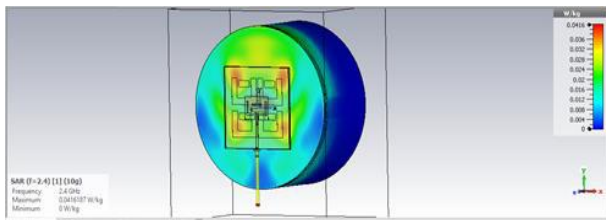


Fig.30 – 10g SAR at 2.4 GHz with the AMC

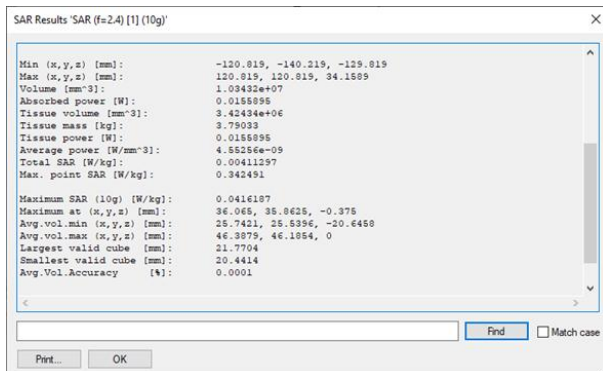


Fig.31 – 10g SAR report at 2.4 GHz

In table 2 a comparison between the antenna with the AMC and without the AMC is presented:

Table 2 – Directivity, Gain and SAR simulated results.
(Limits: ICNIRP 2WKg ANSI 1.6W/Kg).

| Antenna | without AMC F=2,4GHz | with AMC F=2,4GHz |
|-----------------|-------------------------|----------------------|
| Directivity | 5,31 | 9,23 |
| Gain | 1.89 | 6,96 |
| SAR ANSI (1g) | 0,243 | 0,0683 |
| SAR ICNIRP(10g) | 0,120 | 0,0416 |

The results above demonstrate that the proposed antenna system with AMC presented a relevant performance improvement in some characteristics such as: the gain, the directivity and the reduction of SAR when compared to other authors, as shown in Table 3 [2]

Table 3 - Comparison to other authors.

| Parameters | [2] | [8] | [9] | [5] | Este trabalho |
|--------------------------|---------------|---------------|-----------|---------------|---------------|
| Size (mm ²) | 26 X 16 | 30 X 25 | 30 X 30 | 55 X47 | 41X28 |
| Substrate thickness (mm) | 1.5 | 1.6 | 1.6 | 1.2 | 1.6 |
| Substrate | Rogers RO4003 | FR-4 | FR-4 | Rogers RT5880 | FR-4 |
| No. of notches | 2 | 0 | 3 | 2 | 3 |
| Technique applied | Chanfrado | Meia placa | Chanfrado | Chanfrado | Irradiante |
| | 0 0 | L Invertido | com DGS | com DGS | |
| Gain(dBi) | 3.07 | not mentioned | 2.65 | 8.9 | |
| Bandwidth(GHz) | 3.1 - 10 | 1.2 - 12 | 0.91 | 67 | 2.35- 9 |
| Date | 2020 | 2018 | 2020 | 2020 | 2020 |

VIII. CONCLUSION

In this work, a dual-band patch antenna was proposed to reduce the SAR and to operate in the 5G bandwidth. The slot insertion technique was used to establish the frequencies of operation. The evolutionary algorithm CMA-ES was used as a design tool. The development of an unit cell and the 2X2 matrix for the introduction of the metamaterial of the AMC type, produced important results such as 73% increase in the directivity, 71% reduction in the SAR and 268 % increase in the gain, compared to the patch antenna without AMC.

These results can be improved in future works. The application of the CMA-ES evolutionary algorithm together with the AMC matrix, may result in important results further reducing the SAR, as well as improving the antenna gain and the directivity.

ACKNOWLEDGMENTS

The authors are grateful to CNPq and CAPES (financial code 001) Brazilian agencies and for their financial support to part of this work. The authors are also grateful to Norton Soares, Msc Claudio Fernández and Dr. Giovani Bulla for the collaboration to this paper.

REFERENCES

- [1] BALANIS, C. Antenna Theory Analysis and Design. 4.ed., John Wiley & Sons, 2016, 1104p.ISBN 978-1-118-64206-1.
- [2] A. Ejaz, M. Zahid, Y. Amin "Dual Band Notch Planar Patch Antenna for UWB Applications" 2020 3rd International Conference on Computing, Mathematics and Engineering Technologies (iCoMET).
- [3] B. Yin, J. Gu*, X. Feng, B. Wang, Y. Yu, W. Ruan "A Low SAR Value Wearable Antenna for Wireless Body Area Network Based on AMC Structure" Progress In Electromagnetics Research C, Vol. 95, 119–129, 2019
- [4] C. Fernández, G. Bulla, N. Soares, G. Fulgêncio and A. A. de Salles, "Review of Low SAR Antennas for Mobile Applications," 2021 15th European Conference on Antennas and Propagation (EuCAP), pp. 1-5, doi: 10.23919/EuCAP51087.2021.9411305, 2021

- [5] CARVER, K. R.; MINK, J. W. Microstrip antenna technology. IEEE Trans. Antennas Propag., vol. AP-29, Jan 1981, p. 2-24. 153
- [6] DE MORAES ARAÚJO, ALEXANDRE “projeto de antena de microfita com polarização circular para aplicação em veículos aéreos não tripulados” Mossoró - RN Fevereiro, 2018. Dissertação de Mestrado - Universidade Federal Rural do Semi-Árido RN.
- [7] POZAR, D. M.; SCHAUBERT, D. H. Microstrip Antennas - The Analysis and Design of Microstrip Antennas and Arrays. IEEE Press, 1985, ISBN 0-7803-1078-0.
- [8] Ying Zhang, J. von Hagen, M. Younis, C. Fischer, and W. Wiesbeck. Planar artificial magnetic conductors and patch antennas. IEEE Transactions on Antennas and Propagation, 51(10):2704–2712, Oct 2003. 1, 5, 13, 18, 32, 34, 39, 48, 50, 51, 92
- [9] García P, Fernández-Álvarez J. Floquet-Bloch Theory and Its Application to the Dispersion Curves of Nonperiodic Layered. Systems Research Article Vol. 2015 | Article ID 475364 | doi 475364
- [10] U.S. Food and Drug Administration (FDA), Current Research Result on Cell Phones, Washington, DC, USA, updated Mar. 2018.
- [11] Norma IEC/IEEE 62209-1528, AGÊNCIA NACIONAL DE TELECOMUNICAÇÕES ATO Nº 1630, DE 11 DE MARÇO DE 2021. Disponível em: <https://master.org.br/ato-no-1630-atualizacao-dos-procedimentos-de-ensaio-para-sar/> Acesso em 18 out 2021.
- [12] TELECO. Frequências de celular. available: <https://www.teleco.com.br/tutoriais/tutorialrsar/pagina_3.a.sp>. Acesso em: 16 out. 2021.
- [13] S. Kim, I. Nasim “Human Electromagnetic Field Exposure in 5G at 28 GHz” Georgia Southern University DEZ 2020
- [14] N. Hansen, The CMA Evolution Strategy: A Tutorial, Colab Computational Laboratory, Eth Zurich, Icos Institute Of Computational Science, Eth Zurich, June 28, 2011
- [15] G. W. Greenwood, Finding Solutions to NP Problems, Published in proceedings CEC 2001, 815-822, 2001.
- [16] N. Hansen, A. Ostermeier. Adapting arbitrary normal mutation distributions in evolution strategies: The covariance matrix adaptation. In Proceedings of the 1996 IEEE Conference on Evolutionary Computation (ICEC '96), pages 312–317, 1996.
- [17] ICNIRP. ICNIRP Guidelines - For limiting exposure to time-varying electric, magnetic and electromagnetic fields (up to 300 GHz). Disponível em: <https://www.icnirp.org/cms/upload/publications/ICNIRPrfgd12020.pdf>. Acesso em: 18 out. 2021.
- [18] Regulamento sobre limitação da exposição a campos elétricos, magnéticos e eletromagnéticos na faixa de radiofrequências entre 9 kHz e 300 GHz. Anexo à resolução nº 303 de 2 de julho de 2002. ANATEL
- [19] F. Gimán, P. Soh, A. Abdullah “Dual-Band Slot Dipole with AMC using Textiles” International Applied Computational Electromagnetics Society Symposium (ACES 2019)
- [20] D. Ustun, A. Toktas, K. Sabanci, E. Yigit, and F. Toktas, “An UWB Antenna Design Having Band-Reject Characteristic by Y-Shaped Strip,” In IEEE XXIIIrd International Seminar/Workshop on Direct and Inverse Problems of Electromagnetic and Acoustic Wave Theory (DIPED), pp. 185-188, 2018.
- [21] B. Yin, J. Gu, X. Feng, B. Wang, Y. Yu, W. Ruan “A Low SAR Value Wearable Antenna for Wireless Body Area Network Based on AMC Structure” Progress In Electromagnetics Research C, Vol. 95, 119–129, 2019
- [22] <https://www.fcc.gov/general/body-tissue-dielectric-parameters>